ELSEVIER

Journal of Photochemistry and Photobiology A: Chemistry 106 (1997) 75–84

Journal of PHOTOCHEMISTRY AND PHOTOBIOLOGY A: CHEMISTRY

Luminescent coinage metal clusters of acetylides and chalcogenides

Vivian Wing-Wah Yam *

Department of Chemistry, The University of Hong Kong, Pokfulam Road, Hong Kong, Hong Kong

Abstract

A series of polynuclear copper(I) and gold(I) acetylides and tetranuclear copper(I) and silver(I) chalcogenides has been synthesized and shown to exhibit rich photoluminescence behaviour at room temperature. The phosphorescent states of the complexes undergo facile oxidative electron transfer quenching reactions with one-electron pyridinium acceptors and are strong reducing agents in the excited state. An LMCT/d–s mixed state is suggested to be responsible for the low-energy emission. © 1997 Elsevier Science S.A.

Keywords: Acetylides; Chalcogenides; Metal clusters; Photoluminescence

1. Introduction

Increasing interest is being shown in the investigation of luminescent transition metal complexes, other than those with a d^6 metal–diimine core [1,2], which have been studied in detail in recent decades. In particular, polynuclear d^{10} metal complexes have attracted increasing attention in view of their rich photophysical and photochemical behaviour [3–50]. Metal complexes of this class display intriguing structural diversity, since the commonly encountered coordination number around the d^{10} metal centre can vary from two to four with a variety of geometries, the complexity of which increases on increasing the number of metal centres in the polynuclear clusters [51–55]. Another interesting aspect of these polynuclear d^{10} metal complexes is the observation of short metal–metal distances [4,22,23,25,27,31,33,36,40, 45,51–59]. Theoretically, in the absence of metal $(n+1)s$ and $(n+1)p$ functions, the interaction between the closed-shell d^{10} metal centres would be expected to be repulsive in nature. However, configuration mixing of the filled nd orbitals with the empty orbitals derived from higher energy $(n+1)s$ and $(n+1)p$ atomic orbitals converts this repulsion into a slight attraction between the metal centres, giving rise to a weak metal–metal bonding interaction [60–64].

A number of luminescent polynuclear d^{10} metal complexes have been reported to derive their emission from such d–s or d–p excited states originating from weak metal–metal interactions [4,10,11,15,16,19,25,26,30–32,46]. Recently, a number of luminescent polynuclear d^{10} metal complexes have been found to emit from excited states other than that with a pure metal-centred d–s origin. Examples include $[Cu_4I_4(py)_4]$ [6], $[Hg_4(SPh)_6(PPh_3)_4]^{2+}$ [9], $[M_6(mtc)_6]$ (M=Cu, Ag; mtc^-=di-*n*-propylmonothiocarbamate) [5] and $[M_4(SPh)_{10}]^{2-}$ (M=Zn, Cd) [12], which are thought to originate from metal cluster-centred d–s/XLCT or d–s/LMCT mixed states. An analogous $[Ag_4I_4(PPh_3)_4]$ [16] cluster, which exists in both the chair and cubane forms, has also been reported to show interesting luminescence behaviour. However, the luminescence behaviour of the organometallic counterparts has not been explored in detail, despite the large number of organometallic aggregates of coinage metals containing short metal–metal contacts reported in the literature [51–55]. Interest in the bonding picture of these systems has also increased in recent years, and there are examples of metal–metal distances which are even shorter than those found in the metal itself [40,51–55,57–59,65–67]. Discussions on the presence of metal–metal bonding in these systems have been reported, and indicate that a short metal–metal contact does not necessarily reflect the presence of a bonding interaction [51–55].

Following from our recent interest in the luminescence properties of polynuclear d^{10} metal complexes [25–42], we decided that, due to the unusual stereochemistry and various bonding modes of acetylide and unsubstituted chalcogenide ligands, an exploration into the spectroscopic and photophysical behaviour of soluble polynuclear d^{10} metal acetylides and chalcogenide complexes would represent a challenging area of research. Interest in these cluster compounds of high nuclearity has also been stimulated by studies on copper(I)-catalysed organic transformation reactions [52] and on functional models of metal–sulphur redox pro-

* Corresponding author. Tel.: +852 2859 2153; fax: +852 2857 1586; e-mail: wwyam@hkucc.hku.hk.

PII S1010-6030(97)00042-7

teins and metal–chalcogen semiconductor materials [68]. Recent reports on the potential application of metal acetylide complexes as non-linear optical materials have also attracted our attention [69,70]. However, their chemistry has not been studied as extensively as that of the aryl and alkyl counterparts owing to their insolubility in common solvents, which precludes structural characterization studies in many cases. Thus a series of soluble coinage metal acetylide and chalcogenide complexes has been synthesized and structurally characterized: acetylides: $[Cu_3(dppm)_3(\mu_3\text{-}\eta^1\text{-}C{\equiv}CR)]^{2+}$ (R=Ph (**1**), ^{t}Bu (**2**)), $[Cu_3(dppm)_3(\mu_3\text{-}\eta^1\text{-}C{\equiv}CR)_2]^+$ (R=Ph (**3**), ^{t}Bu (**4**)), $[Cu_3(dppm)_3(\mu_3\text{-}\eta^1\text{-}C{\equiv}C^tBu)(\mu_3\text{-}Cl)]^+$ (**5**), $[Cu_4(PAr_3)_4(\mu_3\text{-}\eta^1\text{-}C{\equiv}CPh)_4]$ (Ar=Ph (**6**), C_6H_4-F-*p* (**7**), C_6H_4-Me-*p* (**8**), C_6H_4-OMe-*p* (**9**)), $[Cu_2(PPh_2Me)_4(\mu_2\text{-}\eta^1\text{-}C{\equiv}CPh)_2]$ (**10**), $[Cu_4(PPh_3)_4(\mu_3\text{-}\eta^1,\eta^1,\eta^2\text{-}C{\equiv}CC_6H_4OMe\text{-}p)_3]^+$ (**11**), $[Cu_4(dppm)_4(\mu_4\text{-}\eta^1,\eta^2\text{-}C{\equiv}C\text{-})]^{2+}$ (**12**) and $[Au_4(tppb)(C{\equiv}CR)_4]$ (R=Ph (**13**), C_6H_4-OMe-*p* (**14**), $^nC_6H_{13}$ (**15**)); chalcogenides: $[Cu_4(dppm)_4(\mu_4\text{-}E)]^{2+}$ (E=S (**16**), Se (**17**)) and $[Ag_4(dppm)_4(\mu_4\text{-}E)]^{2+}$ (E=S (**18**), Se (**19**), Te (**20**)) (dppm, bis(diphenylphosphino)methane; tppb, 1,2,4,5-tetrakis(diphenylphosphino)benzene). The structures of complexes **1**–**20** are illustrated in Fig. 1. The photophysical and photochemical properties are reported in Refs. [27–29,33–40].

2. Experimental section

2.1. Materials

All solvents were purified and distilled using standard procedures before use. Organic quenchers for Stern–Volmer quenching experiments and transient absorption spectroscopy were purified by recrystallizing twice using standard procedures.

2.2. Synthesis of coinage metal complexes

All reactions were carried out under anaerobic and anhydrous conditions using standard Schlenk techniques. The metal complexes **1**–**20** were prepared according to the procedures reported previously [27,29,33–40,71–73].

2.3. Physical measurements and instrumentation

UV–visible spectra were obtained on a Hewlett Packard HP8452A diode array spectrophotometer. IR spectra were obtained as Nujol mulls on a Bio-Rad FTS-7 Fourier transform IR spectrophotometer (4000–400 cm^{-1}). Steady state excitation and emission spectra were performed using a Spex Fluorolog-2 111 spectrofluorometer. Low-temperature (77 K) spectra were recorded using an optical Dewar sample holder. Emission lifetime measurements were performed using a conventional laser system. The excitation source was the 355 nm output (third harmonic) of a Quanta-Ray *Q*-switched GCR-150 pulsed Nd-YAG laser. Luminescence decay signals were recorded on a Tektronix model TDS 620A digital oscilloscope and analysed using a program for exponential fitting. All solutions for photophysical studies were prepared under vacuum in a 10 cm^3 round-bottomed flask, equipped with a side-arm 1 cm fluorescence cuvette and sealed from the atmosphere by a Kontes quick-release Teflon stopper. Solutions were rigorously degassed with no fewer than four freeze–pump–thaw cycles.

Time-resolved transient absorption spectroscopy was performed using the 355 nm output (third harmonic) of a Quanta-Ray *Q*-switched GCR-150 pulsed Nd-YAG laser as the excitation source, with the monitoring light beam generated from a 250 W quartz tungsten–halogen lamp placed perpendicular to the excitation beam. The output of the quartz tungsten–halogen lamp was wavelength selected by passing through two monochromators (Oriel 77250, 1/8 m; Oriel 77200, 1/4 m). The transient absorption signals were detected by a Hamamatsu R928 photomultiplier tube; the signal was amplified using a Tektronix AM502 differential amplifier and digitized on a Tektronix model TDS 620A digital oscilloscope, interfaced to an IBM-compatible personal computer for data acquisition and analysis. The transient absorption difference spectra were generated using the point-to-point method. The back electron transfer rate constants (k_{bet}) were obtained from a knowledge of the slope (m) of a plot of the reciprocal of the absorbance change ($1/\Delta A$) vs. time (t) for the transient signal, with $k_{bet} = (\Delta\epsilon)bm$, where $\Delta\epsilon$ is the extinction coefficient difference between the products and reactants at the monitored wavelength and b is the path length of the cell. The plot is linear over at least 2.5 half-lives, indicative of second-order kinetics.

3. Results and discussion

3.1. Copper(I) acetylide complexes

The *triangulo*-Cu_3 complexes **1**–**5** were prepared by the reaction of the binuclear complex $[Cu_2(dppm)_2(MeCN)_2]^{2+}$ [74] with RC≡CH in the presence of KOH or ^{n}BuLi in the appropriate ratio under anaerobic and anhydrous conditions [27,33]. Similar preparations have also been reported by Gimeno and coworkers [71,72]. The complexes consist of an isosceles triangular array of copper atoms with a dppm ligand bridging each edge to form a roughly planar $[Cu_3P_6]$ core. Similarly, the tetranuclear Cu_4 cubane complex **6** was prepared by the reaction of $[Cu(MeCN)_4]^+$, phenylacetylene and an excess of triphenylphosphine and KOH in dichloromethane–methanol under anaerobic and anhydrous conditions. The analogous cubane complexes **7**–**9** were prepared by the depolymerization of $[CuC{\equiv}CPh]_n$ with the respective tertiary phosphines [36,73]. Complex **10** was obtained as yellowish-green crystals by the depolymerization of $[CuC{\equiv}CPh]_n$ with two equivalents of methyldiphenylphosphine in dichloromethane [40]. Complex **11** was

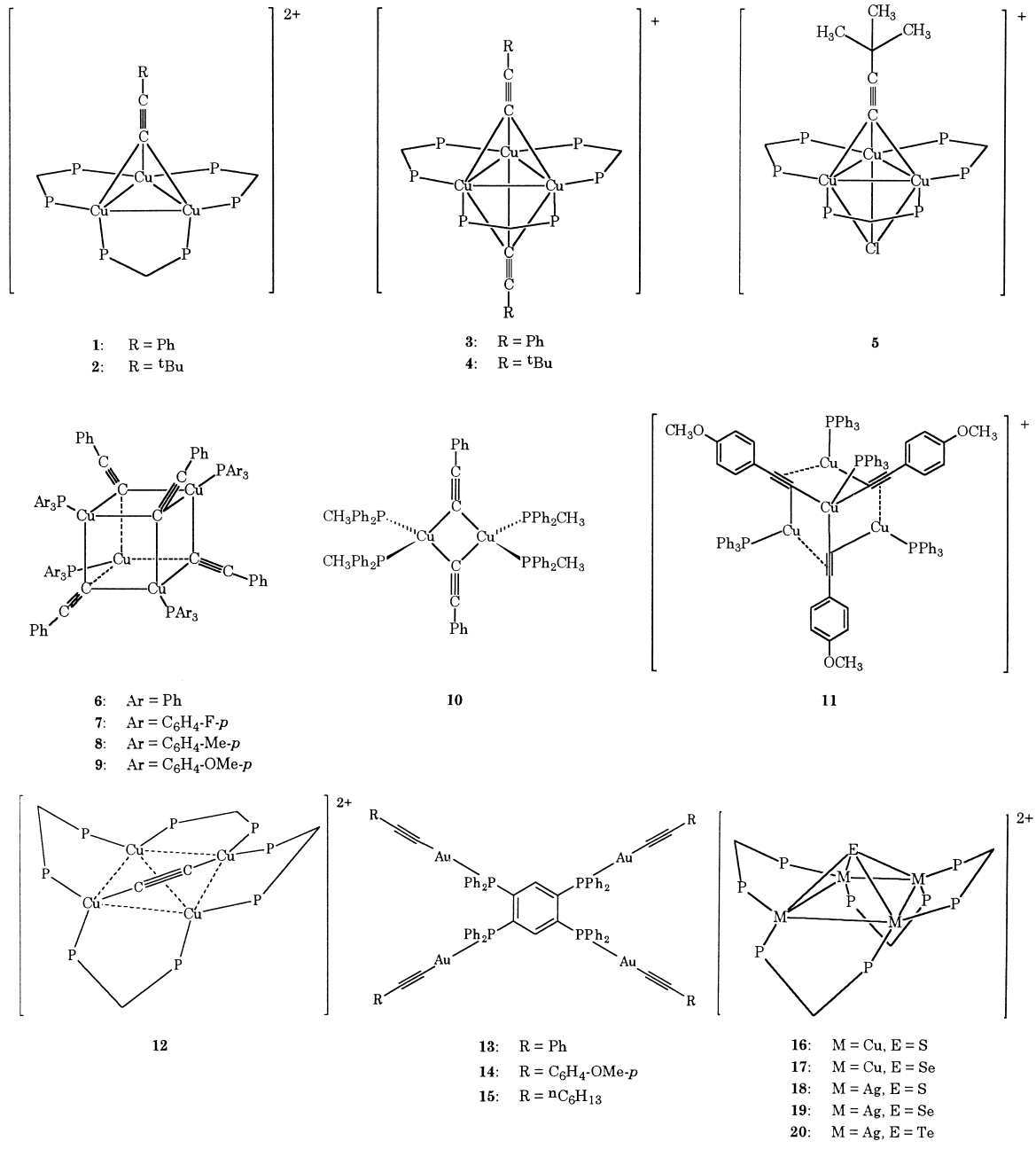

Fig. 1. Structures of complexes **1**–**20**.

prepared by the reaction of $[Cu(MeCN)_4]^+$, triphenylphosphine and [Au(C≡CR)] in dichloromethane [39]. Complex **12** was formed in moderate yield by reaction of $[Cu_2(dppm)_2(MeCN)_2]^{2+}$ with $Me_3SiC{\equiv}CH$ in the presence of ^{n}BuLi in tetrahydrofuran (THF) [37]. A medium sharp peak of the $\nu(C{\equiv}C)$ stretch at approximately 2020 cm^{-1} is observed for complexes **6**–**9**.

The structure of the tetranuclear complexes **6**–**9** consists of an essentially tetrahedral metal skeleton bearing four terminally bonded phosphine molecules and four μ_3-η^1-phenylacetylide ligands. This distorted cubane structure is similar to those observed in other tetranuclear copper(I) clusters, such as $[Cu_4X_4L_4]$ (X=halogen, L=N, P, As donors) [75–77]. The bridging mode of the μ_3-acetylides is asymmetric. The observed C≡C distance and the linearity of the acetylide groups are indicative of a typical C≡C bond and characteristic of metal acetylide σ bonding. Complex **10** is diamond shaped with the acetylide forming a μ_2-η^1 bridge. The structure of complex **11** is essentially similar to that of complexes **6**–**9** except that one of the acetylide vertices is missing. Alternatively, the open-cube Cu_4 complex **11** can be viewed as consisting of a puckered six-membered Cu_3C_3 ring containing Cu(2), Cu(3) and Cu(4), which is reminiscent of the Cu_3S_3 unit, bridged by a $Cu(PPh_3)^+$ unit. Complex **12** shows crystallographic C_2 symmetry, with the four Cu atoms arranged in a distorted rectangular array and the four μ-dppm ligands

Table 1
The Cu–Cu distances for the dinuclear, trinuclear and tetranuclear copper(I) acetylide complexes

Complex	Cu–Cu distance (Å)	Reference
$[Cu_3(dppm)_3(\mu_3\text{-}\eta^1\text{-}C{\equiv}CPh)](BF_4)_2$ (**1**)	2.813(3)–3.274(3)	[72]
$[Cu_3(dppm)_3(\mu_3\text{-}\eta^1\text{-}C{\equiv}C^tBu)](PF_6)_2$ (**2**)	2.910(1)–3.175(1)	[33]
$[Cu_3(dppm)_3(\mu_3\text{-}\eta^1\text{-}C{\equiv}CPh)_2]PF_6$ (**3**)	2.570(3)–2.615(3)	[71,72]
$[Cu_3(dppm)_3(\mu_3\text{-}\eta^1\text{-}C{\equiv}C^tBu)(\mu_3\text{-}Cl)]PF_6$ (**5**)	2.754(2)–2.927(2)	[27]
$[Cu_4(PPh_3)_4(\mu_3\text{-}\eta^1\text{-}C{\equiv}CPh)_4]$ (**6**)	2.523(1)–2.676(1)	[36,73]
$[Cu_4\{P(C_6H_4\text{-}F\text{-}p)_3\}_4(\mu_3\text{-}\eta^1\text{-}C{\equiv}CPh)_4]$ (**7**)	2.550(2)–2.648(2)	[78]
$[Cu_4\{P(C_6H_4\text{-}Me\text{-}p)_3\}_4(\mu_3\text{-}\eta^1\text{-}C{\equiv}CPh)_4]$ (**8**)	2.567(2)–2.607(2)	[36]
$[Cu_2(PPh_2Me)_4(\mu_2\text{-}\eta^1\text{-}C{\equiv}CPh)_2]$ (**10**)	2.454(1)	[40]
$[Cu_4(PPh_3)_4(\mu_3\text{-}\eta^1,\eta^1,\eta^2\text{-}C{\equiv}CC_6H_4OMe\text{-}p)_3]PF_6$ (**11**)	2.446(2)–2.467(2)	[39]
$[Cu_4(dppm)_4(\mu_4\text{-}\eta^1,\eta^2\text{-}C{\equiv}C\text{-})](BF_4)_2$ (**12**)	3.245(2), 3.264(2)	[37]

bridging each of the four Cu–Cu edges in a saddle-like arrangement. The C≡C unit is situated in the middle of the rectangular array of Cu atoms. The Cu–Cu distances for selected complexes are summarized in Table 1. The Cu–Cu distances of complexes **6**–**11** are much shorter than those of the analogous cubane-type copper(I) halide complexes $[Cu(PPh_3)X]_4$ [76]. Indeed, they are similar to or shorter than that observed in metallic copper (2.56 Å). Such short Cu–Cu contacts are not uncommon in organocopper systems [52,53,57–59,67], in particular those of an electron-deficient nature, and may not necessarily indicate significant metal–metal interaction. Complexes **1** and **2** are 44-electron, **3** and **4** 46-electron, **5** 48-electron, **6**–**9** 56-electron, **10** 32-electron and **11** 54-electron systems, and hence all the complexes except **5** are electron deficient.

The electronic absorption data of complexes **1**–**20** are summarized in Table 2. The electronic absorption spectra of complexes **1**–**12** are characterized by a high-energy absorption band at approximately 260 nm and low-energy bands/shoulders in the 300–350 nm region, with a long absorption tail extending to 400–500 nm. The absorption bands at approximately 260 nm are similar to the absorption maxima of the corresponding free phosphine ligands, and are assigned as intraligand transitions. The only absorption spectral feature unique to these clusters is the long-wavelength absorption which tails to 400–500 nm.

Excitation of solid samples or fluid solutions of **1**–**12** at $\lambda > 350$ nm produces a long-lived intense dual luminescence. The photophysical data are collected in Table 3. Selected emission spectra of complexes **1**–**12** are shown in Figs. 2–4. The low-temperature (77 K) solid state emission spectra of complexes **1**–**6** and **11** show very similar patterns: a high-energy band at approximately 440–495 nm and a lower energy emission at about 525–700 nm. The high-energy emis-

Table 2
The electronic absorption data for complexes **1**–**20**

Complex	λ nm (ϵ_{max} dm^3 mol^{-1} cm^{-1}) [a]
$[Cu_3(dppm)_3(\mu_3\text{-}\eta^1\text{-}C{\equiv}CPh)](BF_4)_2$ (**1**)	260 sh (41450), 330 sh (14290) [b]
$[Cu_3(dppm)_3(\mu_3\text{-}\eta^1\text{-}C{\equiv}C^tBu)](PF_6)_2$ (**2**)	260 sh (40890), 330 sh (2120) [b]
$[Cu_3(dppm)_3(\mu_3\text{-}\eta^1\text{-}C{\equiv}CPh)_2]PF_6$ (**3**)	255 sh (48825), 305 sh (32390) [b]
$[Cu_3(dppm)_3(\mu_3\text{-}\eta^1\text{-}C{\equiv}C^tBu)_2]PF_6$ (**4**)	255 sh (39280), 350 sh (6150) [b]
$[Cu_3(dppm)_3(\mu_3\text{-}\eta^1\text{-}C{\equiv}C^tBu)(\mu_3\text{-}Cl)]PF_6$ (**5**)	255 sh (42170), 330 sh (6950) [b]
$[Cu_4(PPh_3)_4(\mu_3\text{-}\eta^1\text{-}C{\equiv}CPh)_4]$ (**6**)	261 (71300), 386 (17150), 445 (10675) [c]
$[Cu_4\{P(C_6H_4\text{-}F\text{-}p)_3\}_4(\mu_3\text{-}\eta^1\text{-}C{\equiv}CPh)_4]$ (**7**)	260 (69790), 310 (31965), 400 (7305) [c]
$[Cu_4\{P(C_6H_4\text{-}Me\text{-}p)_3\}_4(\mu_3\text{-}\eta^1\text{-}C{\equiv}CPh)_4]$ (**8**)	260 (86405), 320 (36750), 400 (7710) [c]
$[Cu_4\{P(C_6H_4\text{-}OMe\text{-}p)_3\}_4(\mu_3\text{-}\eta^1\text{-}C{\equiv}CPh)_4]$ (**9**)	260 (133210), 320 (41210), 400 (7735) [c]
$[Cu_2(PPh_2Me)_4(\mu_2\text{-}\eta^1\text{-}C{\equiv}CPh)_2]$ (**10**)	248 (51515), 315 (15290) [c]
$[Cu_4(PPh_3)_4(\mu_3\text{-}\eta^1,\eta^1,\eta^2\text{-}C{\equiv}CC_6H_4OMe\text{-}p)_3]PF_6$ (**11**)	252 sh (88550), 330 (48925) [c]
$[Cu_4(dppm)_4(\mu_4\text{-}\eta^1,\eta^2\text{-}C{\equiv}C\text{-})](BF_4)_2$ (**12**)	262 (62580), 374 sh (6900) [b]
$[Au_4(tppb)(C{\equiv}CPh)_4]$ (**13**)	241 sh (138455), 271 sh (102320), 365 sh (9400) [c]
$[Au_4(tppb)(C{\equiv}CC_6H_4\text{-}OMe\text{-}p)_4]$ (**14**)	262 sh (133850), 276 (133895), 288 sh (126185), 302 sh (103260), 370 sh (10945) [c]
$[Au_4(tppb)(C{\equiv}CC_6H_{13})_4]$ (**15**)	289 sh (37715), 355 sh (5620) [c]
$[Cu_4(dppm)_4(\mu_4\text{-}S)](PF_6)_2$ (**16**)	265 sh (41490), 285 sh (34650) [b]
$[Cu_4(dppm)_4(\mu_4\text{-}Se)](PF_6)_2$ (**17**)	262 sh (42670) [b]
$[Ag_4(dppm)_4(\mu_4\text{-}S)](OTf)_2$ (**18**)	246 sh (91745), 400 sh (970) [b]
$[Ag_4(dppm)_4(\mu_4\text{-}Se)](OTf)_2$ (**19**)	256 sh (53985), 402 sh (1445) [b]
$[Ag_4(dppm)_4(\mu_4\text{-}Te)](OTf)_2$ (**20**)	254 sh (67075), 440 sh (1475) [b]

[a] From Refs. [27,29,33–40].
[b] In MeCN at 298 K.
[c] In CH_2Cl_2 at 298 K.

Table 3
Photophysical data for complexes **1**–**12** [a]

Complex	Medium (T K)	λ_{em} nm (τ_0 μs)
1	Solid (298)	500 (21 ± 2)
	Solid (77)	492, 530 sh
	Me_2CO (298)	499 (6.8 ± 0.7)
	MeCN (298)	499 (15 ± 1)
2	Solid (298)	627 (14 ± 1)
	Solid (77)	450, 570 sh, 692
	Me_2CO (298)	640 (2.6 ± 0.3)
3	Solid (298)	493 (14 ± 1)
	Solid (77)	485, 525 sh
	^{n}PrCN glass (77)	471, 500 sh
	Me_2CO (298)	495 (5.9 ± 0.5)
	MeCN (298)	494 (6.5 ± 0.6)
4	Solid (298)	450 (0.44 ± 0.05), 540 (1.7 ± 0.2)
	Solid (77)	450, 530 sh
	^{n}PrCN glass (77)	442, 500 sh
	Me_2CO (298)	444 (0.24 ± 0.02), 580 sh (16 ± 1)
	MeCN (298)	456 (0.27 ± 0.03), 600 sh (4.1 ± 0.4)
5	Solid (298)	440 sh (< 0.01), 535 (33 ± 3)
	Solid (77)	440, 572
	MeCN (298)	540 sh (5.3 ± 0.5), 613 (5.4 ± 0.5)
6	Solid (298)	483 sh (3.7 ± 0.3), 522 (3.7 ± 0.3)
	Solid (77)	477, 524
	CH_2Cl_2 (298)	420, 520 sh (< 0.01), 616 (3.6 ± 0.3)
7	Solid (298)	516 (1.3 ± 0.1)
	Solid (77)	516
	CH_2Cl_2 (298)	420, 510 sh, 606 (0.86 ± 0.09)
8	Solid (298)	548 (0.52 ± 0.05)
	Solid (77)	535
	CH_2Cl_2 (298)	410, 510 sh, 620
9	Solid (298)	529 (2.9 ± 0.3)
	Solid (77)	521
	CH_2Cl_2 (298)	410, 670
10	Solid (298)	467, 509 (87 ± 5)
	Solid (77)	464, 511
	CH_2Cl_2 (298)	529, 660 sh
11	Solid (298)	445, 630 sh (20.7 ± 1.0)
	Solid (77)	445
	CH_2Cl_2 (298)	675 (2.7 ± 0.3)
	Me_2CO (298)	675 (4.0 ± 0.4)
12	Solid (298)	509 (9.8 ± 0.9)
	Solid (77)	551
	Me_2CO (298)	562 (16 ± 1)
	MeCN (298)	560 (2.9 ± 0.3)

[a] From Refs. [27,33,36,37,39,40].

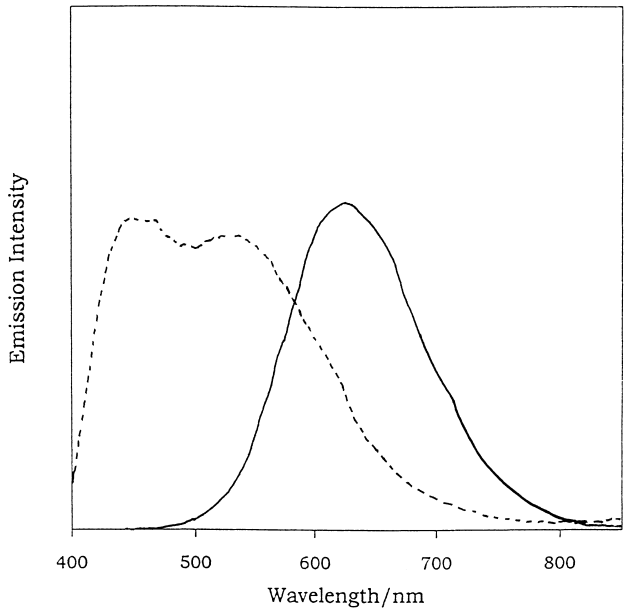

Fig. 2. Solid state emission spectra of complexes **2** (———) and **4** (- - -) at room temperature. Excitation wavelength, 350 nm.

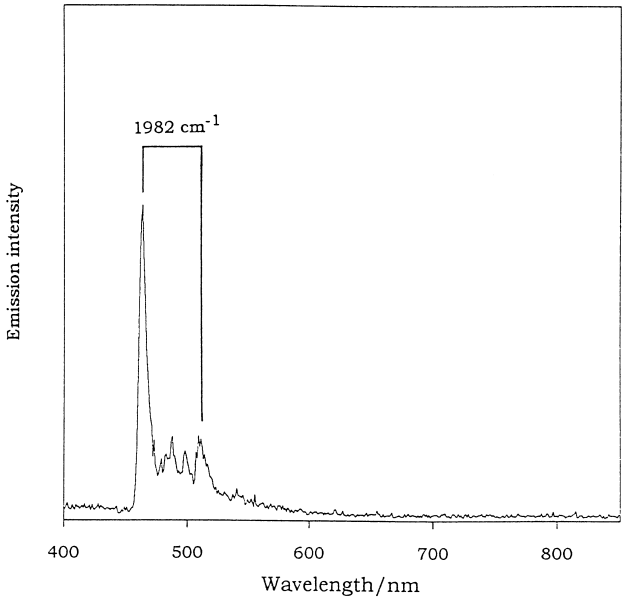

Fig. 3. Solid state emission spectrum of complex **10** at 77 K. Excitation wavelength, 350 nm.

sion is probably due to either metal-to-ligand charge transfer ($Cu \rightarrow \pi^*(RC{\equiv}C^-)$ MLCT) or intraligand transition ($\pi \rightarrow \pi^*(RC{\equiv}C^-)$ IL), since complexes **2**, **4** and **5** emit at similar energies (450 nm for **2** and **4**, 440 nm for **5**), whereas the emission of **1**, **3** and **6** occurs at lower energy (492 nm for **1**, 485 nm for **3** and 483 nm for **6**), consistent with the lower π^* energy level for the phenylacetylide moiety. The low-energy emission at approximately 525–700 nm is probably associated with a spin-forbidden transition, given the long lifetime of the emission observed. It is possible that the low-energy emitting state is related to the metal-centred excited state $3d^9 4s^1$ of Cu(I), modified by the copper–copper interaction, due to configuration mixing of the filled orbitals of d parentage with the appropriate empty orbitals derived from the higher energy 4s and 4p atomic orbitals of the trimeric or tetrameric copper unit (d–s). A more probable assignment of the origin of the low-energy emission involves an acetylide-to-metal charge transfer ($RC{\equiv}C^- \rightarrow Cu_3$ LMCT for complexes **1**–**5**, $RC{\equiv}C^- \rightarrow Cu_4$ LMCT for complexes **6**–**9** and **11**, $RC{\equiv}C^- \rightarrow Cu_2$ LMCT for complex **10** and $C{\equiv}C^{2-} \rightarrow Cu_4$ LMCT for complex **12**) excited state [27,33,36,37,39,40]. The close resemblance between the emission energies of the cubane complexes **6**–**9** and the dia-

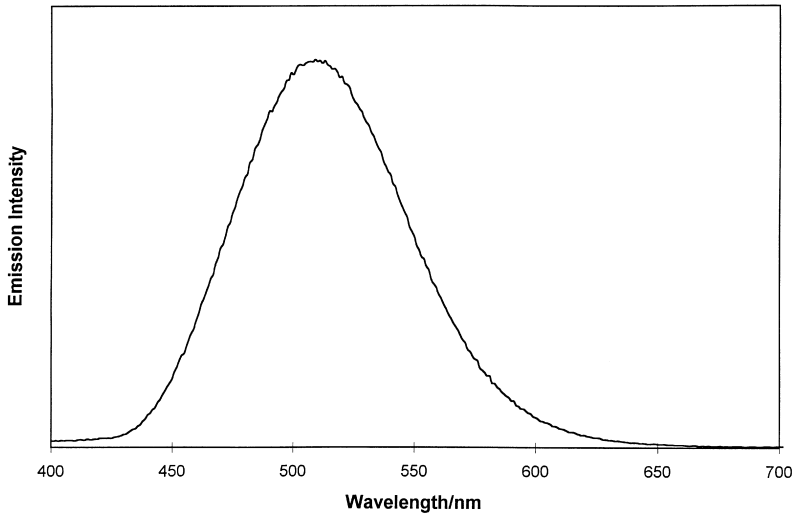

Fig. 4. Solid state emission spectrum of complex **12** at room temperature. Excitation wavelength, 350 nm.

mond complex **10** further supports an LMCT assignment with a lower degree of d–s character. Similar assignments have been suggested for tetrameric iodocopper(I) clusters [4,6,7]. In this context, we believe that, with complexes **2**, **4**, and **5**, where the strongly σ-donating $^{t}BuC{\equiv}C^{-}$ is involved, the low-energy emission probably derives from an LMCT/d–s mixed state with predominantly LMCT character. This has been suggested on the grounds that the low-energy emission band displays solvatochromism, with its energy shifted to the blue on going from acetonitrile to the less polar solvent acetone, indicative of charge transfer nature, and the low-energy emission band in **2** is red shifted relative to those observed in **4** and **5**. This is consistent with the fact that **2**, carrying an overall charge of 2+, would render the metal centre more readily reducible. A pure d–s origin would predict that **2** would emit at higher energy, owing to the larger Cu–Cu distances in the monocapped system relative to the mixed halide-acetylide capped and bicapped systems (Table 1). The red shift in the emission energy of **2** relative to **4** and **5** is also in accord with that expected for an LMCT assignment with decreasing coordination number. For complexes **1** and **3**, the low-energy emission also probably derives from an LMCT/d–s mixed state [27,33].

Similarly, a red shift in energy of the low-energy emission band from 616 nm in complex **6** to 675 nm in complex **11** in dichloromethane is consistent with the assignment of an LMCT/d–s origin. This is in line with the better σ-donating ability of the *p*-methoxyphenylacetylide moiety as well as the fact that complex **11**, bearing an overall positive charge of 1+, would render the metal centre more readily reducible. A similar assignment of an LMCT/d–s origin has been suggested for the low-energy emission of complex **12** [37].

It is interesting to note that, regardless of the nature of the excited state (d–s, LMCT or LMCT/d–s admixture), the lowest energy transition would involve the promotion of an electron to an empty bonding s orbital, i.e. the LUMO would remain σ bonded with regard to the metal cluster core, resulting in an excited state which is strongly contracted and distorted owing to an increase in Cu–Cu bonding in this state [4]. Such a distortion would be one of the factors accounting for the large Stokes shifts observed in these Cu(I) complexes.

The phosphorescent state of complexes **1**–**5**, **11** and **12** has been found to be quenched by a number of pyridinium acceptors. Since the triplet state energy of pyridinium ion is too high for the occurrence of any appreciable energy transfer reaction between the excited state of the complex and the quencher, the quenching mechanism is probably due to electron transfer. A representative non-linear least-squares fit of a plot of the logarithm of the bimolecular quenching rate constant vs. the reduction potential of the pyridinium acceptor for complex **11** is shown in Fig. 5. Table 4 summarizes the excited state reduction potentials of selected tetranuclear copper(I) complexes estimated from Stern–Volmer quenching studies using a series of structurally related pyridinium acceptors with varying reduction potentials. The electron transfer nature of these quenching reactions was further confirmed by nanosecond transient absorption spectroscopy. A representative transient absorption difference spectrum generated from the laser flash photolysis of a degassed acetone solution (0.1 M $^{n}Bu_4NPF_6$) of complex **4** and 4-methoxycarbonyl-*N*-methylpyridinium hexafluorophosphate is shown in Fig. 6. All spectra were dominated by a high-energy band at approximately 400 nm and a much broader band at about 790–850 nm [28,33]. The 400 nm band is characteristic of pyridinyl radicals and matches well the reported spectrum of the reduced radical of 4-methoxycarbonyl-*N*-methylpyridinium [79,80]. The 790–850 nm band (λ_{max} nm (ϵ_{max} dm^3 mol^{-1} cm^{-1}): **3**, 810 (9990); **4**, 790 (8480); **5**, 830 (7900)) does not originate from the pyridinyl radical, but should be characteristic of the polynuclear copper acetylide cluster.

The mechanism for the reaction of the phosphorescent state of the trinuclear Cu(I) acetylide complexes with 4-methoxycarbonyl-*N*-methylpyridinium ion probably occurs as shown below

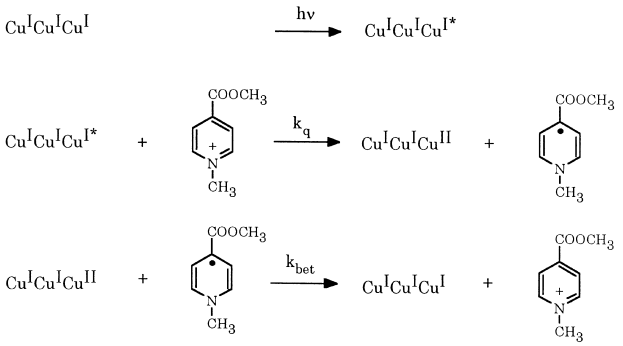

It is probable that the 790–850 nm absorption is a result of the mixed-valence $Cu^ICu^ICu^{II}$ species and can be attributed to an intervalence transfer (IT) transition [28,33,81–83]

$$[Cu^ICu^ICu^{II}] \xrightarrow{h\nu} [Cu^ICu^{II}Cu^I]^*$$

The back electron transfer rate constants (k_{bet}) are estimated to be 2.3×10^{10}, 1.7×10^{10} and 2.7×10^{10} dm^3 mol^{-1} s^{-1} for the reaction of 4-methoxycarbonyl-*N*-methylpyridinyl radical with $[\mathbf{3}]^+$, $[\mathbf{4}]^+$ and $[\mathbf{5}]^+$ respectively.

3.2. Gold(I) acetylide complexes

Reaction of $[Au(C{\equiv}CR)]_n$ with 0.25 equivalent of tppb in CH_2Cl_2 afforded the desired complexes $[Au_4(tppb)(C{\equiv}CR)_4]$ (**13**, R=Ph; **14**, R=C_6H_4OMe-*p*; **15**, R=$^nC_6H_{13}$) in high yield [38]. Short intramolecular Au–Au contacts of 3.1541(4) Å are observed between adjacent Au units in complex **13**. The electronic absorption spectra show intense absorption bands at 250–300 nm with a lower energy shoulder at approximately 365 nm (Table 2).

Excitation of the complexes at $\lambda > 350$ nm in the solid state and in dichloromethane solutions results in a long-lived intense emission (Table 5), the origin of which is suggested to be dominated by the involvement of the bridging tppb ligand [38].

Table 4
The excited state reduction potentials of the tetranuclear copper(I) complexes

Complex	Excited state reduction potential (V vs. SSCE)	Reference
11	−1.71(10)	[39]
12	−1.77(10)	[37]
16	−1.72(10)	[29]
17	−1.55(10)	[34]

The phosphorescent state has also been found to undergo facile oxidative quenching reactions with pyridinium acceptors, such as methyl viologen, confirmed by transient absorption spectroscopy. A back electron transfer rate constant of 1.94×10^{10} dm^3 mol^{-1} s^{-1} has been obtained.

3.3. Copper(I) and silver(I) chalcogenides

Complexes **16**–**20** were prepared by the reaction of $[M_2(dppm)_2(MeCN)_2]^{2+}$ with Na_2E or Li_2E (M=Cu, E=S, Se; M=Ag, E=S, Se, Te) in acetone [29,34,35]. They are isostructural, with the four metal atoms arranged in a distorted rectangular array bridged by a μ_4-E atom. Unlike complex **12**, where the C≡C unit is situated in the middle of the rectangle, the chalcogen atom is projected above the M_4 plane occupying the apex of a distorted rectangular-based pyramid. The four bridging dppm ligands are arranged in a saddle-like configuration as in complex **12**. The metal–metal contacts are summarized in Table 6. The Cu–Cu distances in complex **16** are slightly shorter than those found in complex **17**. Similarly, the Ag–Ag distances also increase slightly in the order **18** < **19** < **20**, a trend expected with increasing size of the atom from S to Se to Te. It is interesting to note that the Cu–Cu distances in complexes **16** and **17** are shorter than those found in complex **12**, which is understandable on the grounds that the C≡C unit is larger in size and is situated on

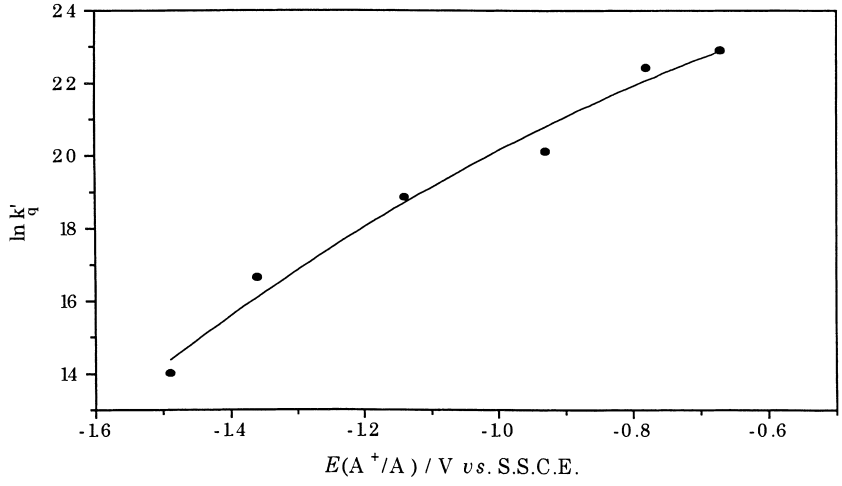

Fig. 5. Plot of ln k'_q vs. $E(A^+/A)$ for the electron transfer quenching of complex **11** by pyridinium acceptors in degassed acetone.

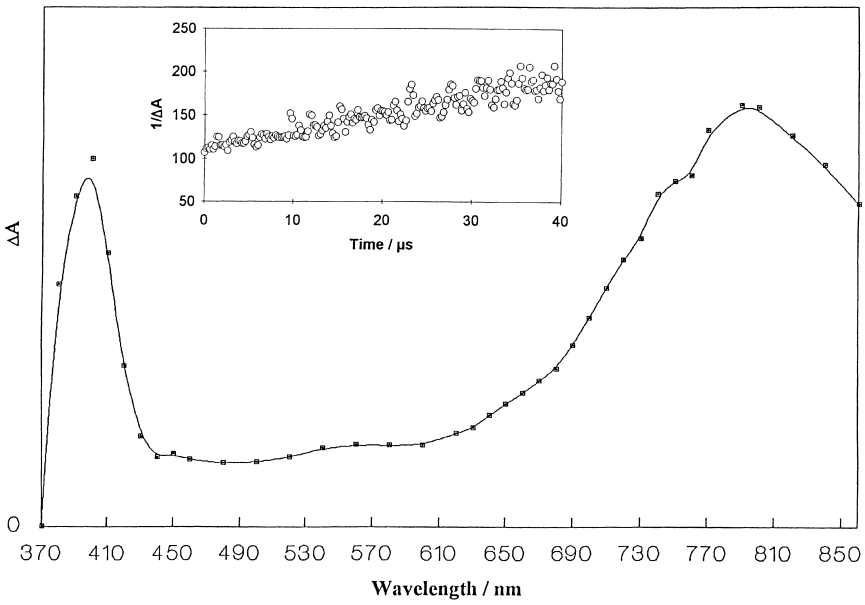

Fig. 6. Transient absorption difference spectrum recorded 10 μs after laser flash excitation of a degassed acetonitrile solution of complex **4** (1.0×10^{-4} M) and 4-methoxycarbonyl-*N*-methylpyridinium ion (1.3×10^{-2} M). The inset shows a plot of $1/\Delta A$ monitored at 400 nm vs. time.

Table 5
Photophysical data for gold(I) acetylide complexes [a]

Complex	Medium (T K)	λ_{em} nm (τ_0 μs)
13	Solid (298)	599[b], 611[c] (0.57)
	Solid (298)[d]	529[b] (2.52)
	Solid (77)	584[b], 611[c]
	Solid (77)[d]	529[b], 569[c]
	CH_2Cl_2 (298)	510, 538 sh[b] (0.46)
14	Solid (298)	415[b], 628[c] (1.85)
	Solid (77)	414[b], 618[c]
	CH_2Cl_2 (298)	447, 601[b] (0.47)
15	Solid (298)	405, 602[b] (1.28)
	Solid (77)	586[b]
	CH_2Cl_2 (298)	409, 577[b] (0.71)

[a] From Ref. [38].
[b] Excitation wavelength, 350 nm.
[c] Excitation wavelength, 450 nm.
[d] Crystalline non-ground samples were used for the measurements.

Table 6
The metal–metal distances for copper(I) and silver(I) chalcogenides

Complex	M–M distance (Å)	Reference
16	2.869(1), 3.128(1)	[29]
17	2.908(4), 3.271(4)	[34]
18	3.038(2), 3.160(2)	[35]
19	3.055(2), 3.222(2)	[35]
20	3.071(1), 3.357(1)	[35]

the plane of the Cu_4 core and inevitably pushes the Cu atoms further apart in complex **12**.

The electronic absorption spectra of complexes **16**–**20** display a high-energy absorption shoulder at approximately 260 nm, attributable to intraligand transition of the dppm ligand, and low-energy absorptions in the 330–450 nm region (Table 2). On excitation of the complexes at $\lambda > 350$ nm, an intense green to orange emission is observed. The emission spectra are shown in Figs. 7 and 8. The photophysical data are summarized in Table 7. On the basis of the good σ-

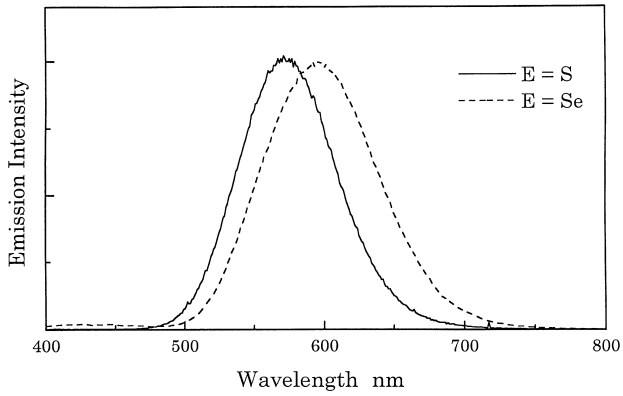

Fig. 7. Solid state emission spectra of complexes **16** and **17** at room temperature. Excitation wavelength, 350 nm.

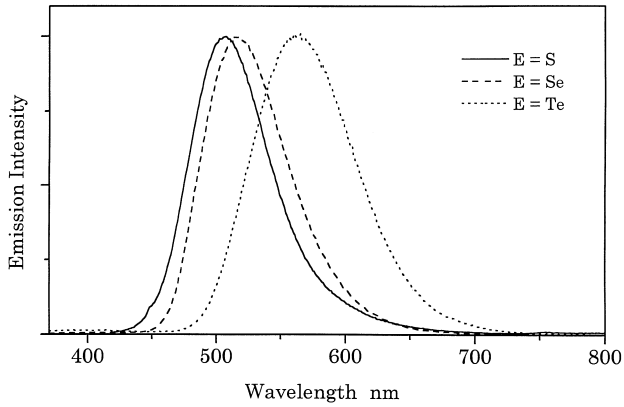

Fig. 8. Solid state emission spectra of complexes **18**–**20** at room temperature. Excitation wavelength, 350 nm.

Table 7
Photophysical data for copper(I) and silver(I) chalcogenides [a]

Complex	Medium (T K)	λ_{em} nm (τ_0 μs)
16	Solid (298)	579 (3.6 ± 0.1)
	Solid (77)	606
	MeCN (298)	618 (7.8 ± 0.2)
	Me_2CO (298)	622 (8.1 ± 0.2)
17	Solid (298)	595 (3.9 ± 0.2)
	Solid (77)	619
	MeCN (298)	622 (6.9 ± 0.2)
	Me_2CO (298)	626 (7.1 ± 0.2)
18	Solid (298)	516 (1.0 ± 0.1)
	Solid (77)	536
	MeCN (298)	628 (1.5 ± 0.2)
	Me_2CO (298)	628 (1.2 ± 0.1)
19	Solid (298)	527 (0.9 ± 0.1)
	Solid (77)	552
	MeCN (298)	572 (3.4 ± 0.3)
	Me_2CO (298)	570 (1.3 ± 0.1)
20	Solid (298)	574 (3.1 ± 0.2)
	Solid (77)	588
	MeCN (298)	626 (3.3 ± 0.3)
	Me_2CO (298)	615 (1.4 ± 0.1)

[a] From Refs. [29,34,35].

donating ability of the chalcogenide ion, the transitions probably originate predominantly from an LMCT ($E^{2-} \rightarrow M_4$) triplet excited state, perhaps with mixing of a metal-centred (d–s/d–p) state. The energies of the solid state luminescence follow the order **16** > **17** and **18** > **19** > **20**, in line with the changes in the ionization potentials of the chalcogens, and hence the σ-donating effect of the chalcogenide ions. A comparison of the emission energies of the Cu(I) complexes with their Ag(I) analogues also reveals the trend **16** < **18** and **17** < **19**, again in line with the LMCT assignment. Molecular orbital calculation results [84,85] also reveal a chalcogenide-based HOMO, with some contribution from the metal centres, and an essentially metal-localized LUMO, confirming the assignment of the excited state as an admixture of LMCT ($E^{2-} \rightarrow M_4$) and metal-centred (d–s/d–p) states [29,34,35].

The phosphorescence of complexes **16**–**20** has been found to be quenched by a number of pyridinium acceptors via an oxidative electron transfer mechanism. The excited state reduction potentials estimated from quenching experiments using a series of structurally related quenchers are collected in Table 4. The electron transfer nature of the reactions has been confirmed by transient absorption spectroscopy. The transient absorption difference spectra of the reaction of complex **16** with pyridinium acceptors show absorption bands at approximately 400 and 690 nm. The former is the characteristic absorption of the pyridinyl radical. The latter is probably a result of the mixed-valence $Cu^{I}Cu^{I}Cu^{I}Cu^{II}$ species and is attributed to an IT transition.

Acknowledgements

V.W.W.Y. acknowledges financial support from the Research Grants Council and The University of Hong Kong.

References

[1] V. Balzani, F. Scandola, Supramolecular Photochemistry, Ellis Horwood, Chichester, 1991.
[2] O. Horváth, K.L. Stevenson, Charge Transfer Photochemistry of Coordination Compounds, VCH, New York, 1993.
[3] D.M. Knotter, G. Blasse, J.P.M. van Vliet, G. van Koten, Inorg. Chem. 31 (1992) 2196.
[4] P.C. Ford, A. Vogler, Acc. Chem. Res. 26 (1993) 220.
[5] F. Sabin, C.K. Ryu, P.C. Ford, A. Vogler, Inorg. Chem. 31 (1992) 1941.
[6] K.R. Kyle, P.C. Ford, J. Am. Chem. Soc. 111 (1989) 5005.
[7] C.K. Ryu, M. Vitale, P.C. Ford, Inorg. Chem. 32 (1993) 869, and references cited therein.
[8] H. Kunkely, A. Vogler, J. Chem. Soc., Chem. Commun. (1990) 1204.
[9] H. Kunkely, A. Vogler, Chem. Phys. Lett. 164 (1989) 621.
[10] A. Vogler, H. Kunkely, Chem. Phys. Lett. 150 (1988) 135.
[11] A. Vogler, H. Kunkely, Chem. Phys. Lett. 158 (1989) 74.
[12] T. Türk, U. Resch, M.A. Fox, A. Vogler, Inorg. Chem. 31 (1992) 1854.
[13] T. Türk, U. Resch, M.A. Fox, A. Vogler, J. Phys. Chem. 96 (1992) 3818.
[14] A. Avdeef, J.P. Fackler Jr., Inorg. Chem. 17 (1978) 2182.
[15] C. King, J.C. Wang, Md.N.I. Khan, J.P. Fackler Jr., Inorg. Chem. 28 (1989) 2145, and references cited therein.
[16] M. Henary, J.I. Zink, Inorg. Chem. 30 (1991) 3111.
[17] M. Henary, J.I. Zink, J. Am. Chem. Soc. 111 (1989) 7407.
[18] S.D. Hanna, J.I. Zink, Inorg. Chem. 35 (1996) 297.
[19] P.D. Harvey, F. Adar, H.B. Gray, J. Am. Chem. Soc. 111 (1989) 1312.
[20] T.M. McCleskey, H.B. Gray, Inorg. Chem. 31 (1992) 1733.
[21] N.P. Rath, E.M. Holt, K. Tanimura, J. Chem. Soc., Dalton Trans. (1986) 2303, and references cited therein.
[22] H.R.C. Jaw, M.M. Savas, R.D. Rogers, W.R. Mason, Inorg. Chem. 28 (1989) 1028.
[23] H.R.C. Jaw, M.M. Savas, W.R. Mason, Inorg. Chem. 28 (1989) 4366.
[24] W.B. Jones, J. Yuan, R. Narayanaswamy, M.A. Young, R.C. Elder, A.E. Bruce, M.R.M. Bruce, Inorg. Chem. 34 (1995) 1996.
[25] V.W.W. Yam, T.F. Lai, C.M. Che, J. Chem. Soc., Dalton Trans. (1990) 3747.
[26] V.W.W. Yam, W.K. Lee, J. Chem. Soc., Dalton Trans. (1993) 2097.
[27] V.W.W. Yam, W.K. Lee, T.F. Lai, Organometallics 12 (1993) 2383.
[28] V.W.W. Yam, W.K. Lee, P.K.Y. Yeung, D. Phillips, J. Phys. Chem. 98 (1994) 7545.
[29] V.W.W. Yam, W.K. Lee, T.F. Lai, J. Chem. Soc., Chem. Commun. (1993) 1571.
[30] D. Li, C.M. Che, H.L. Kwong, V.W.W. Yam, J. Chem. Soc., Dalton Trans. (1992) 3325.
[31] C.M. Che, H.K. Yip, V.W.W. Yam, P.Y. Cheung, T.F. Lai, S.J. Shieh, S.M. Peng, J. Chem. Soc., Dalton Trans. (1992) 427.
[32] C.M. Che, H.L. Kwong, C.K. Poon, V.W.W. Yam, J. Chem. Soc., Dalton Trans. (1990) 3215.
[33] V.W.W. Yam, W.K. Lee, K.K. Cheung, B. Crystall, D. Phillips, J. Chem. Soc., Dalton Trans. (1996) 3283.
[34] V.W.W. Yam, K.W.W. Lo, K.K. Cheung, Inorg. Chem. 35 (1996) 3459.
[35] V.W.W. Yam, K.W.W. Lo, C.R. Wang, K.K. Cheung, Inorg. Chem. 35 (1996) 5116.
[36] V.W.W. Yam, W.K. Lee, K.K. Cheung, J. Chem. Soc., Dalton Trans. (1996) 2335.
[37] V.W.W. Yam, W.K.M. Fung, K.K. Cheung, Angew. Chem., Int. Ed. Engl. 35 (1996) 1100.
[38] V.W.W. Yam, S.W.K. Choi, K.K. Cheung, Organometallics 15 (1996) 1734.
[39] V.W.W. Yam, S.W.K. Choi, C.L. Chan, K.K. Cheung, Chem. Commun. (1996) in press.
[40] V.W.W. Yam, W.K. Lee, K.K. Cheung, H.K. Lee, W.P. Leung, J. Chem. Soc., Dalton Trans. (1996) 2889.

[41] V.W.W. Yam, S.W.K. Choi, K.K.W. Lo, W.F. Dung, R.Y.C. Kong, J. Chem. Soc., Chem. Commun. (1994) 2379.
[42] V.W.W. Yam, S.W.K. Choi, J. Chem. Soc., Dalton Trans. (1994) 2057.
[43] S.J. Shieh, H. Xiao, S.M. Peng, C.M. Che, J. Chem. Soc., Dalton Trans. (1994) 3067.
[44] H. Xiao, K.K. Cheung, C.X. Guo, C.M. Che, J. Chem. Soc., Dalton Trans. (1994) 1867.
[45] C.M. Che, H.K. Yip, W.C. Lo, S.M. Peng, Polyhedron 13 (1994) 887.
[46] C.M. Che, H.K. Yip, D. Li, S.M. Peng, G.H. Lee, Y.M. Wang, S.T. Liu, J. Chem. Soc., Chem. Commun. (1991) 1615.
[47] B.C. Tzeng, D. Li, S.M. Peng, C.M. Che, J. Chem. Soc., Dalton Trans. (1993) 2365.
[48] C.K. Chan, K.K. Cheung, C.M. Che, J. Chem. Soc., Chem. Commun. (1996) 227.
[49] C.F. Wang, S.M. Peng, C.K. Chan, C.M. Che, Polyhedron 15 (1996) 1853.
[50] R. Beer, G. Calzaferri, I. Kamber, J. Chem. Soc., Chem. Commun. (1991) 1489.
[51] A. Grohmann, H. Schmidbaur, in: E.W. Abel, F.G.A. Stone, G. Wilkinson (Eds.), Comprehensive Organometallic Chemistry II, vol. 3, Pergamon, Oxford, 1995, pp. 1–56.
[52] G. van Koten, S.L. James, J.T.B.H. Jastrzebski, in: E.W. Abel, F.G.A. Stone, G. Wilkinson (Eds.), Comprehensive Organometallic Chemistry II, vol. 3, Pergamon, Oxford, 1995, pp. 57–133.
[53] B.J. Hathaway, in: G. Wilkinson, R.D. Gillard, J.A. McCleverty (Eds.), Comprehensive Coordination Chemistry, vol. 5, Pergamon, Oxford, 1987, pp. 533–774.
[54] R.J. Lancashire, in: G. Wilkinson, R.D. Gillard, J.A. McCleverty (Eds.), Comprehensive Coordination Chemistry, vol. 5, Pergamon, Oxford, 1987, pp. 775–859.
[55] R.J. Puddephatt, in: G. Wilkinson, R.D. Gillard, J.A. McCleverty (Eds.), Comprehensive Coordination Chemistry, vol. 5, Pergamon, Oxford, 1987, pp. 861–923.
[56] G. Jia, R.J. Puddephatt, I.D. Scott, J.J. Vittal, Organometallics 12 (1993) 3565.
[57] S. Gambarotta, C. Floriani, A. Chiesi-Villa, C. Guastini, J. Chem. Soc., Chem. Commun. (1983) 1156.
[58] J.A.J. Jarvis, B.T. Kilbourn, R. Pearce, M.F. Lappert, J. Chem. Soc., Chem. Commun. (1973) 475.
[59] X. He, M.M. Olmstead, P.P. Power, J. Am. Chem. Soc. 114 (1992) 9668.
[60] Y. Jiang, S. Alvarez, R. Hoffmann, Inorg. Chem. 24 (1985) 749.
[61] K.M. Merz Jr., R. Hoffmann, Inorg. Chem. 27 (1988) 2120.
[62] J.P. Fackler Jr., Prog. Inorg. Chem. 21 (1976) 55.
[63] P.K. Mehrotra, R. Hoffmann, Inorg. Chem. 17 (1978) 2187.
[64] D.M.P. Mingos, J. Chem. Soc., Dalton Trans. (1976) 1163.
[65] J.C. Slater, J. Chem. Phys. 41 (1964) 3199.
[66] R.I. Papasergio, C.L. Raston, A.H. White, J. Chem. Soc., Chem. Commun. (1983) 1419.
[67] A.J. Edwards, M.A. Paver, P.R. Raithby, M.A. Rennie, C.A. Russell, D.S. Wright, Organometallics 13 (1994) 4967.
[68] A. Müller, B. Krebs, Sulfur. Its Significance for Chemistry for the Geo-, Bio- and Cosmosphere and Technology, Elsevier, Amsterdam, 1984.
[69] H.B. Fyfe, M. Mlekuz, G. Stringer, N.J. Taylor, T.B. Marder, in: R.M. Laine (Ed.), Inorganic and Organometallic Polymers with Special Properties, Kluwer Academic, Netherlands, 1992, pp. 331–344.
[70] N.J. Long, Angew. Chem., Int. Ed. Engl. 34 (1995) 21.
[71] J. Diéz, M.P. Gamasa, J. Gimeno, A. Aguirre, S. García-Granda, Organometallics 10 (1991) 380.
[72] J. Diéz, M.P. Gamasa, J. Gimeno, E. Lastra, A. Aguirre, S. García-Granda, Organometallics 12 (1993) 2213.
[73] L. Naldini, F. Demartin, M. Manassero, M. Sansoni, G. Rassu, M.A. Zoroddu, J. Organomet. Chem. C 42 (1985) 279.
[74] J. Diéz, M.P. Gamasa, J. Gimeno, A. Tiripicchio, M.T. Camellini, J. Chem. Soc., Dalton Trans. (1987) 1275.
[75] C.L. Raston, A.H. White, J. Chem. Soc., Dalton Trans. (1976) 2153.
[76] J.C. Dyason, P.C. Healy, L.M. Engelhardt, C. Pakawatchai, V.A. Patrick, C.L. Raston, A.H. White, J. Chem. Soc., Dalton Trans. (1985) 831.
[77] M.R. Churchill, W.J. Young, Inorg. Chem. 18 (1979) 1133, and references cited therein.
[78] V.W.W. Yam, K.K. Cheung, unpublished result, 1996.
[79] J. Hermolin, M. Levin, E.M. Kosower, J. Am. Chem. Soc. 103 (1981) 4808.
[80] J. Hermolin, M. Levin, Y. Ikegami, M. Sawayanagi, E.M. Kosower, J. Am. Chem. Soc. 103 (1981) 4795.
[81] R.R. Gagné, C.A. Koval, T.J. Smith, M.C. Cimolino, J. Am. Chem. Soc. 101 (1979) 4571.
[82] M.E. Barr, P.H. Smith, W.E. Antholine, B. Spencer, J. Chem. Soc., Chem. Commun. (1993) 1649.
[83] C. Harding, V. McKee, J. Nelson, J. Am. Chem. Soc. 113 (1991) 9684.
[84] C.R. Wang, K.K.W. Lo, V.W.W. Yam, Chem. Phys. Lett. 262 (1997) 91.
[85] C.R. Wang, K.K.W. Lo, V.W.W. Yam, J. Chem. Soc., Dalton Trans. (1997) 227.